Appl. Phys. A (2015) 120:1399–1406
DOI 10.1007/s00339-015-9324-8

Applied Physics A
Materials Science & Processing

A molecular dynamics study on the vibration of carbon and boron nitride double-walled hybrid nanotubes

R. Ansari[1] · **S. Ajori**[1]

Received: 7 April 2015 / Accepted: 24 June 2015 / Published online: 2 July 2015

Abstract Synthesis of hybrid nanotubes to overcome the drawbacks of individual pure nanotubes in order to apply them in novel nanodevices has attracted great interest of researchers. To this end, pure single- and double-walled boron nitride nanotubes together with carbon and boron nitride double-walled hybrid nanotubes are simulated through molecular dynamics simulations in order to study their vibrational behavior. The natural frequency of nanotubes is computed, and the effects of geometrical parameters and boundary conditions on the natural frequency are investigated. According to the generated results, the natural frequency of boron nitride nanotubes is higher than that of their carbon counterpart and nanotubes with clamped boundary conditions possess the highest natural frequency compared to other types of boundary conditions. Also, the natural frequency of double-walled hybrid nanotubes is found to be between those of pure double-walled boron nitride and carbon nanotubes with small lengths. It is found that the natural frequency of double-walled hybrid nanotubes is less sensitive to length increase compared to pure double-walled carbon and boron nitride ones, leading to higher frequencies at greater lengths. Finally, to study the variation in natural frequency with the length, a rational curve is fitted to each data set and the corresponding constants are computed.

✉ S. Ajori
Shahram_ajori1366@yahoo.com

[1] Department of Mechanical Engineering, University of Guilan, P.O. Box 3756, Rasht, Iran

1 Introduction

The discovery of the most important tubular nanostructures in 1990s, i.e., carbon nanotubes (CNTs) [1, 2] and boron nitride nanotubes (BNNTs) [3, 4], has begun a new era in nanoscience and nanotechnology. Numerous experimental and theoretical investigations have evidenced comparable mechanical properties of CNTs and BNNTs despite the electrical and thermochemical properties. These properties make them so promising in fabricating novel nanoelectromechanical systems (NEMS) [5–8]. CNTs are found to be metallic and semiconducting depending on their radius and chirality [9–16]. On the contrary, BNNTs behave as an insulator with a wide band gap of $\sim$6 eV [10, 12, 14, 15] making it suitable for nanocables [17–20]. Also, it is observed that BNNTs possess higher thermal stability and chemical inertness compared to CNTs [10, 12, 13]. These considerable differences between the two nanotubes result in proposing hybrid carbon and boron nitride nanotubes since the earlier attempts of doping carbon nanotubes with boron and nitrogen [21] in order to overcome the drawbacks in applying the individual pure CNTs and BNNTs in novel applications. To this end, many efforts have been made to fabricate carbon and boron nitride hybrid nanotubes since 1994 [22–29]. Regarding the developments in experimental growth of hybrid nanotubes, several theoretical and experimental investigations have been carried out to explore the electromagnetic properties and stability of these hybrid nanotubes unlike the mechanical properties which are limited to elastic properties [30–34]. Although these studies have explored some crucial properties of hybrid nanotubes, it is important to understand their mechanical behavior as they are applied to any NEMS. According to the published literature, a limited number of studies have been performed on the vibrational behavior of

pure CNTs and BNNTs, free or torsional, employing molecular dynamics (MD) simulations and continuum theories [35–42]. In this regard, a comprehensive study is made to investigate the vibrational behavior (free vibration) of carbon and boron nitride double-walled hybrid nanotubes through MD simulations which has not been considered so far. Finally, the natural frequency is obtained and the effects of geometrical parameters, different boundary conditions and formation configurations on the natural frequency are investigated.

2 Methodology

To perform MD simulations, a homemade computer code is prepared by MATLAB®. To this end, the Tersoff–Brenner [43, 44] and the Tersoff-like [45, 46] empirical potential energy functions are employed to calculate bonded energy of CNTs and BNNTs, respectively. Also, the vdW interaction energy between the walls of the nanotubes is simulated through the Lennard–Jones (LJ) pairwise potential energy function [47, 48] as non-bonded energy function. Finally, the total potential energy of system is obtained by summing the bonded and non-bonded energies of system, i.e., Tersoff–Brenner, Tersoff-like and the LJ potential energies. Also, velocity Verlet algorithm [49] is employed to integrate the equations of motions at the basic time step of 1 fs together with Nose–Hoover thermostat algorithm in order to control temperature of system at the room temperature (300 K) in the canonical ensemble [50]. Applying this thermostat leads to less fluctuation of system during thermal stabilization [51].

To simulate different boundary conditions such as simply supported (SS) and clamped (CC), one and four rows of atoms are fixed, respectively [39–42], as demonstrated in Fig. 1. In order to obtain equilibrium structure and optimal energy, the system is initially relaxed up to 10 ps. Afterward, nanotubes are deformed to their initial mode of vibration and then allowed to vibrate freely for a specific time which is dependent on the size of system. Note that to simulate the vibration of nanotubes, the boundary atoms are selected to be the thermostat atoms. Finally, the histories of the center of mass of nanotubes are saved and natural frequency is calculated using fast Fourier transform (FFT).

3 Results and discussion

To study the vibrational behavior of carbon and boron nitride double-walled hybrid nanotubes, (5,5) and (10,10) single-walled and (5,5)@(10,10) double-walled nanotubes

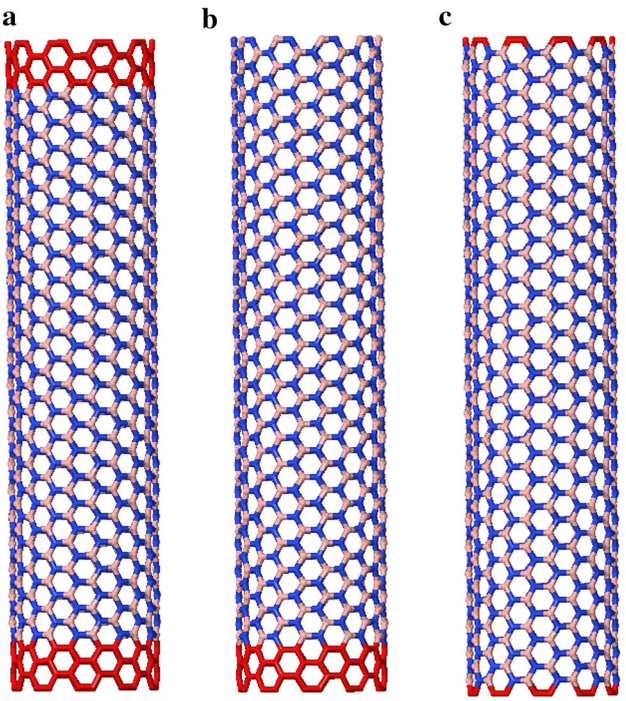

Fig. 1 Schematic representation of SWBNNTs with **a** CC, **b** CF and **c** SS boundary conditions

are chosen with different lengths varying from 25 to 120 Å. It should be noted that as the results of natural frequency are approximately insensitive to chirality [39], only armchair nanotubes are taken into considerations. According to the published literature, due to the lack of data regarding to free vibration of BNNTs, to validate the generated code, Young's modulus of BNNTs can be determined by incorporating the calculated natural frequency of BNNTs into continuum theory relation between Young's modulus and axial frequency in the case of axial vibration of BNNT with clamped–free (CF) boundary condition, as follows [52, 53]:

$$f = \frac{(2n-1)\sqrt{\frac{E}{\rho}}}{4L}, \quad n = 1, 2, \ldots \tag{1}$$

where f is axial frequency, E is Young's modulus, and ρ indicates density given by:

$$\rho = \frac{M}{\pi DtL} \tag{2}$$

To perform the axial vibration, a (5,5) BNNT with the length of 60 Å and CF boundary condition is selected and small axial displacement is applied to the free end of nanotube, and then it is allowed to vibrate. The histories of center of mass of BNNT are stored, and the time response of BNNT is plotted in Fig. 2. Throughout FFT, the frequency is obtained around 0.72 THz. By substituting the obtained axial frequency into Eq. (1), Young's modulus of

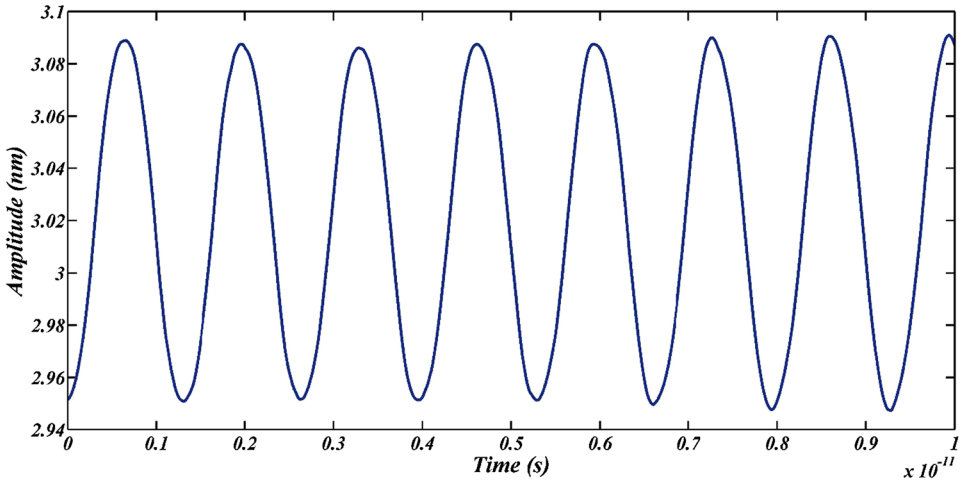

Fig. 2 A sample of time response for axial vibration of BNNT

0.9 TPa is obtained which is in good agreement with previously published data [54–56].

Considering free vibration of BNNTs, Fig. 3 presents the effects of different boundary conditions on the natural frequency of BNNTs. As it is observed, the frequency of clamped BNNTs with similar lengths is higher than that of BNNTs with SS and CF boundary conditions. The highest frequency belongs to BNNT with the length of 22 Å and CC boundary condition. Changing the type of boundary conditions from CC to SS and CF causes approximately 24 and 65 % reduction in the natural frequency, respectively. This discrepancy reduces to 10 % in the case of BNNTs with SS boundary condition as the length increases to 120 Å, whereas it remains approximately constant for CF boundary conditions as the length increases.

In order to more precisely study the variation in natural frequency of BNNTs with the length by a simple mathematical model, rational curve fitting is performed according to the following equation:

$$f(x) = \frac{ax + b}{x + c} \tag{3}$$

where f indicates natural frequency of BNNTs in THz, and a, b and c represent constants in THz, THz.Å and Å, respectively. Employing a curve fitting technique, the constants are calculated. Table 1 presents the values of aforementioned constants for (10,10) BNNT. As demonstrated, a and c are negative, while b is positive and, all these constants qualitatively guarantee the reduction of frequency as the length increases. This reduction is around 94 % for all boundary conditions.

In order to explore the effect of nanotube radius on the natural frequency, Fig. 4 is depicted for BNNTs with CC boundary conditions. For a specific length, it can be seen that nanotubes with higher diameters possess higher frequencies. According to the calculated data, the natural frequency of (10,10) BNNT at the length of 22 Å is around 1.1 times higher than that of (5,5) BNNT, whereas it

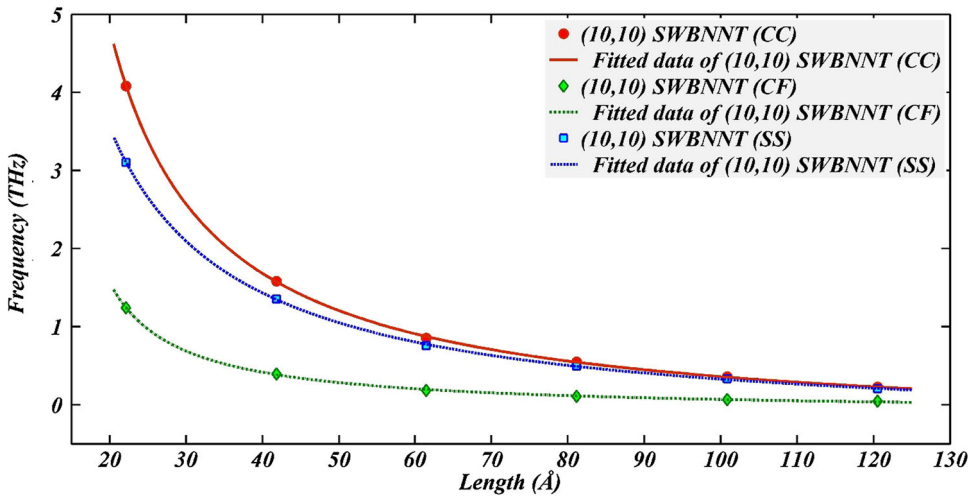

Fig. 3 Effects of different boundary conditions on the natural frequency of SWBNNT

Table 1 Values of constants for Eq. (1) corresponding to (10,10) SWBNNT with different boundary conditions

Chirality and boundary conditions	*a*	*b*	*c*
(10,10), (CC)	−0.3683	70.35	−6.91
(10,10), (CF)	−0.1002	16.05	−11.01
(10,10), (SS)	−0.3503	66.73	−3.145

Table 2 Values of constants for Eq. (1) corresponding to (5,5) SWBNNT with CC boundary conditions

Chirality and boundary conditions	*a*	*b*	*c*
(5,5) (CC)	−0.4178	60.48	−8.207

reaches 1.9 times as the length increases up to 120 Å. Further, the constants of Eq. (3) are computed and presented in Table 2 for (5,5) BNNT with CC boundary conditions. Comparison between the values of *a*, *b* and *c* related to (5,5) and (10,10) BNNTs demonstrates that nanotubes with smaller radii possess lower values compared to bigger nanotubes. Considering the diameter, by increasing the diameter, the moment of inertia increases. The order of this increase is more pronounced than that of cross section. Also, according to [57], mass density decreases as the tube diameter increases. So, according to direct and reverse dependence of natural frequency on the moment of inertia and mass density [53], respectively, for a similar length, tube with higher diameter possesses higher natural frequency.

To make a comparison between the natural frequencies of CNTs and their inorganic analogous, i.e., BNNTs, Fig. 5 is illustrated. To this end, two (10,10) carbon and boron nitride nanotubes are chosen and boundaries are taken to be CC. According to the results, the natural frequency of BNNTs is higher than that of CNTs. This difference is around 27 % at the length of 22 Å, and it rises to 36 % as the length of nanotube increases up to 120 Å. It should be noted that the natural frequency of CNTs obtained in this study is in complete agreement with previously published data [39, 42]. Comparing the density of C–C and B–N, it can be found that C–C is denser than B–N in hexagonal sp^2 hybridized structure. According to [57], the density of (10,10) SWCNT of greater than 3 g/cm^3 is obtained, which is considerably higher than that of B–N hexagonal structure obtained around 2.1 g/cm^3. This is the essential reason for higher frequency of BNNTs compared to CNTs. Also, from chemical bonding point of view, unlike the B–N hexagonal structure, the presence of powerful double bonds in hexagonal structure of CNTs can affect the vibration behavior and reduce the natural frequency of CNTs compared to that of BNNTs.

To investigate the effect of number of walls on the natural frequency, (5,5)@(10,10) double-walled BNNT (DWBNNT) is taken with CC boundary conditions. As demonstrated in Fig. 6, the natural frequency of DWBNNT is between those of individual inner and outer constituent nanotubes, i.e., (5,5) and (10,10). Moreover, it can be seen that natural frequencies are converged to each other as the length increases enough. These results are qualitatively similar to those reported in the previously published works on CNTs [39].

Finally, the vibrational behaviors of carbon and boron nitride double-walled hybrid nanotubes are explored. To this end, two types of double-walled hybrid nanotubes are simulated, i.e., a (5,5) single-walled CNT (SWCNT) inside a (10,10) single-walled BNNT (SWBNNT), (CNT@BNNT) and vice versa (BNNT@CNT) which are depicted in Fig. 7. The boundaries are taken to be CC, natural frequencies are calculated, and Fig. 8 is presented. According to this figure, in the case of smaller nanotubes up to 50 Å, DWBNNTs possess the highest frequency compared to double-walled hybrid nanotubes and DWCNTs and natural frequency of

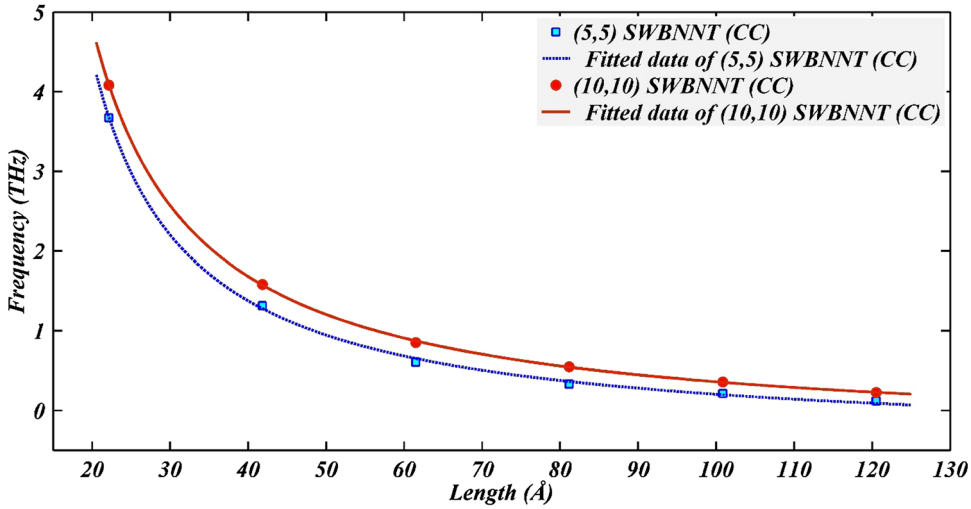

Fig. 4 Effect of tube radius on the natural frequency of SWBNNT

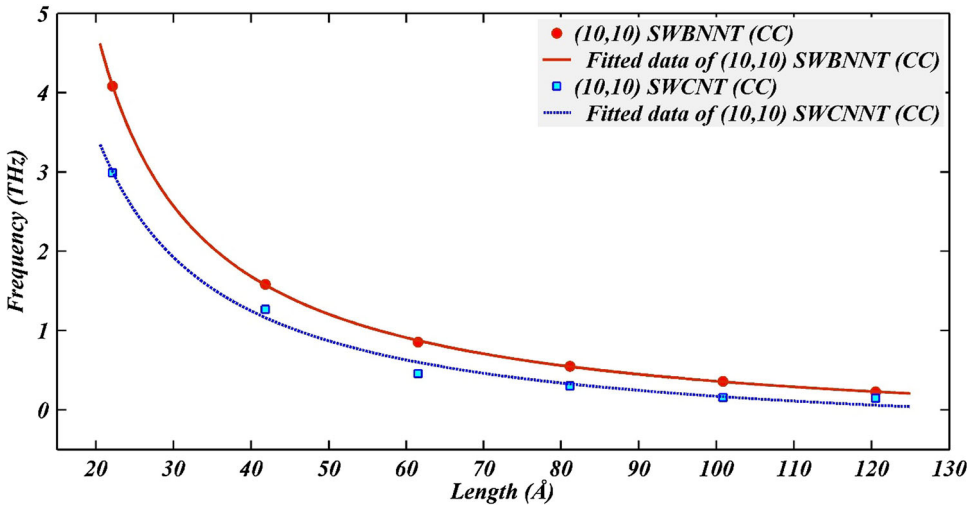

Fig. 5 Effect of material type on the natural frequency of nanotubes in the case of carbon and boron nitride

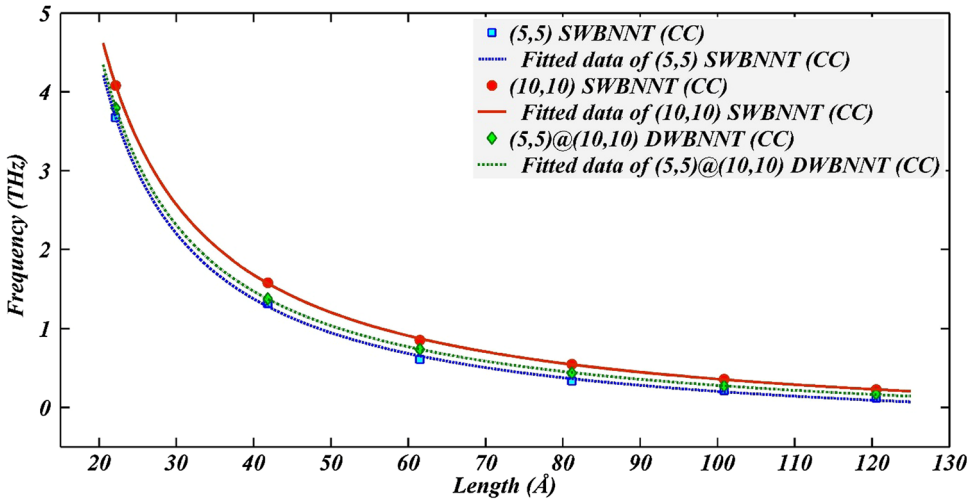

Fig. 6 Effect of the number of walls on the natural frequency of BNNTs

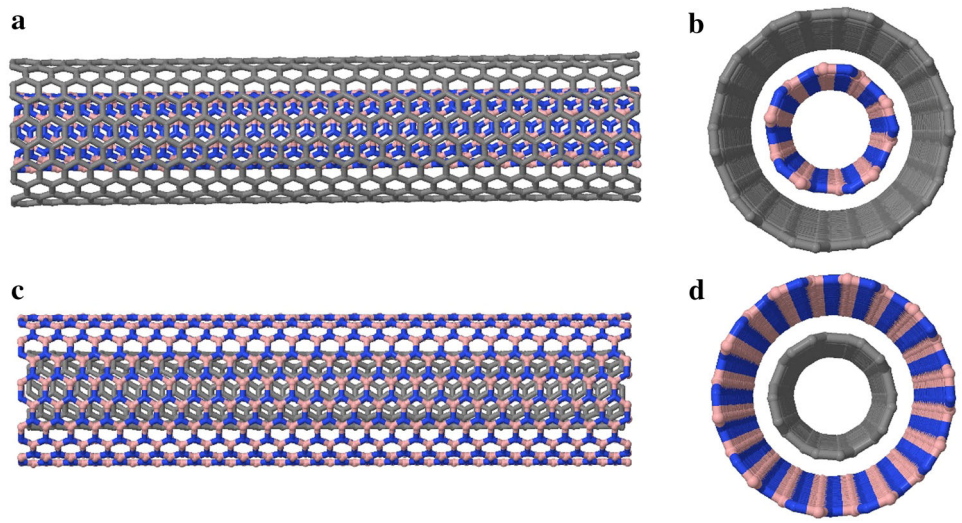

Fig. 7 Molecular models of CNT@BNNT and BNNT@CNT double-walled hybrid nanotubes

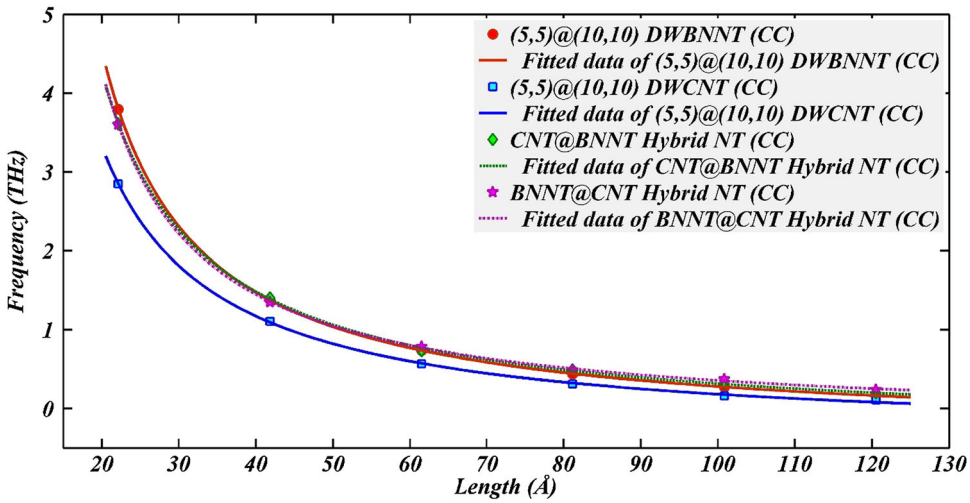

Fig. 8 Comparison of the variation of natural frequencies for DWBNNT, DWCNT and double-walled hybrid nanotubes

Table 3 Values of constants for Eq. (1) corresponding to DWBNNT, DWCNTs and double-walled hybrid nanotubes with CC boundary conditions

Type	*a*	*b*	*c*
DWBNNT	−0.3558	61.25	−8.075
DWCNT	−0.3876	55.93	−5.516
CNT@BNNT	−0.3273	62.08	−6.955
BNNT@CNT	−0.2204	54.7	−8.303

double-walled hybrid nanotubes lies between those of pure DWBNNTs and DWCNTs. As the length increases, the natural frequency of double-walled hybrid nanotubes with BNNT inside CNT (BNNT@CNT) reduces less than that of other nanostructures. This results in higher natural frequency of BNNT@CNT compared to that of DWBNNTs and DWCNTs as the length increases. Note that the highest frequency belongs to BNNT@CNT double-walled hybrid nanotubes. It can be concluded that natural frequency of double-walled hybrid nanotubes is less sensitive to the length variation at greater lengths as it is compared to pure double-walled nanotubes. It should be noted that for both types of double-walled hybrid nanotubes at the smaller lengths, computed frequencies are close together. For example, at the length of 22 Å, the difference between the natural frequencies of CNT@BNNT and BNNT@CNT is around 0.3 %, whereas it increases to 16 % at the length of 120 Å. Finally, the constants of Eq. (1) are computed and presented in Table 3.

4 Conclusion

In this investigation, MD simulations were employed to simulate vibrational behavior of single- and double-walled BNNT and double-walled hybrid nanotubes. The natural frequency was computed and the effects of geometrical parameters and boundary conditions were studied. The results demonstrated that nanotubes with clamped boundary conditions have higher natural Frequencies in comparison with other types of boundary conditions. Also, it was observed that the natural frequency of BNNT is larger than that of its carbon counterpart, and the natural frequency of DWBNNT is between those of its constituent inner and outer nanotubes with the same length and boundary conditions; considering the double-walled carbon and boron nitride hybrid nanotubes, it was seen that their natural frequency is between those of pure DWBNNT and DWCNTs with the same length and boundary conditions at smaller lengths. Furthermore, it was shown that, as the length increases, the reduction rate of natural frequencies related to double-walled nanotubes is quicker than that related to double-walled hybrid nanotubes leading to higher frequencies of double-walled hybrid nanotubes compared to pure ones. Finally, in order to study the variation in natural frequency with the length, rational curve was fitted to data of frequency and the constants corresponding to each data set were computed.

References

1. S. Iijima, Helical microtubules of graphitic carbon. Nature **354**, 56 (1991)
2. T.W. Ebbesen, P.M. Ajayan, H. Hiura, K. Tanigaki, Purification of nanotubes. Nature **358**, 220 (1992)
3. A. Rubio, J.L. Corkill, M.L. Cohen, Theory of graphitic boron nitride nanotubes. Phys. Rev. B **49**, R5081 (1994)
4. N.G. Chopra, R.L. Luyken, K. Cherrey, V.H. Crespi, M.L. Cohen, S.G. Louie, A. Zettl, Boron-nitride nanotubes. Science **269**, 966 (1995)
5. J.M. Schnorr, T.M. Swager, Emerging applications of carbon nanotubes. Chem. Mater. **23**, 646 (2011)

6. M.F.L. De Volder, S.H. Tawfick, R.H. Baughman, A.J. Hart, Carbon nanotubes: present and future commercial applications. Science **339**, 535 (2013)
7. M. Terrones, Science and technology of the twenty-first century: synthesis, properties, and applications of carbon nanotubes. Annu. Rev. Mater. Res. **33**, 419 (2003)
8. S. Park, M. Vosguerichian, Z. Bao, A review of fabrication and applications of carbon nanotube film-based flexible electronics. Nanoscale **5**, 1727 (2013)
9. J.W.G. Wilder, L.C. Venema, A.G. Rinzler, R.E. Smalley, C. Dekker, Electronic structure of atomically resolved carbon nanotubes. Nature **391**, 59 (1998)
10. R. Arenal, X. Blase, A. Loiseau, Boron-nitride and boron carbon nitride nanotubes: synthesis, characterization and theory. Adv. Phys. **59**, 101 (2010)
11. D. Golberg, Y. Bando, C.C. Tang, C.Y. Zhi, Boron nitride nanotubes. Adv. Mater. **19**, 2413–2432 (2007)
12. P. Ayala, R. Arenal, A. Loiseau, A. Rubio, T. Pichler, The physical and chemical properties of heteronanotubes. Rev. Mod. Phys. **82**, 1843–1885 (2010)
13. Y.K. Yap, *B-C–N Nanotubes and Related Nanostructures* (Springer, Dordrecht, 2009)
14. A. Rubio, J.L. Corkill, M.L. Cohen, Theory of graphitic boron nitride nanotubes. Phys. Rev. B **49**, 5081–5084 (1994)
15. X. Blase, A. Rubio, S.G. Louie, M.L. Cohen, Stability and band gap constancy of boron-nitride nanotubes. Europhys. Lett. **28**, 335–340 (1994)
16. R. Arenal, O. Stephan, M. Kociak, D. Taverna, A. Loiseau, C. Colliex, Electron energy loss spectroscopy measurement of the optical gaps on individual boron nitride single-walled and multiwalled nanotubes. Phys. Rev. Lett. **95**, 127601 (2005)
17. R. Ma, D. Golberg, Y. Bando, T. Sasaki, Syntheses and properties of B-C–N and BN nanostructures. Phil. Trans. R. Soc. Lond. A **362**, 2161–2186 (2004)
18. R. Ma, Y. Bando, T. Sato, Coaxial nanocables: Fe nanowires encapsulated in BN nanotubes with intermediate C layers. Chem. Phys. Lett. **350**, 1 (2001)
19. Y. Bando, K. Ogawa, D. Goldberg, Insulating 'nanocables': invar Fe–Ni alloy nanorods inside BN nanotubes. Chem. Phys. Lett. **347**, 349 (2001)
20. D. Golberg, F.F. Xu, Y. Bando, Filling boron nitride nanotubes with metals. Appl. Phys. A **76**, 479 (2003)
21. O. Stephan, P.M. Ajayan, C. Colliex, P. Redlich, J.M. Lambert, P.M. Bernier, P. Lefin, Doping graphitic and carbon nanotube structures with boron and nitrogen. Science **266**, 1683 (1994)
22. K. Suenaga, C. Colliex, N. Demoncy, A. Loiseau, H. Pascard, F. Willaime, Synthesis of nanoparticles and nanotubes with well-separated layers of boron nitride and carbon. Science **278**, 653 (1997)
23. R. Arenal, A. Lopez-Bezanilla, In situ formation of carbon nanotubes encapsulated within boron nitride nanotubes via electron irradiation. ACS Nano **8**, 8419 (2014)
24. R. Nakanishi, R. Kitaura, J.H. Warner, Y. Yamamoto, S. Arai, Y. Miyata, H. Shinohara, Thin single-wall BN-nanotubes formed inside carbon nanotubes. Sci. Rep. **3**, 1385 (2013)
25. W. Mickelson, S. Aloni, W.Q. Han, J. Cumings, A. Zettl, Packing C_{60} in boron nitride nanotubes. Science **300**, 467 (2003)
26. A. Trave, F.J. Ribeiro, S.G. Louie, M.L. Cohen, Energetics and structural characterization of C_{60} polymerization in BN and carbon nano peapods. Phys. Rev. B **70**, 205418 (2004)
27. S. Enouz, O. Stephan, J.L. Cochon, C. Colliex, A. Loiseau, C−BN patterned single-walled nanotubes synthesized by laser vaporization. Nano Lett. **7**, 1856 (2007)
28. W.L. Wang, X.D. Bai, K.H. Liu, Z. Xu, D. Golberg, Y. Bando, E.G. Wang, Direct synthesis of B−C−N single-walled nanotubes by bias-assisted hot filament chemical vapor deposition. J. Am. Chem. Soc. **128**, 6530 (2006)
29. X. Wei, M.S. Wang, Y. Bando, D. Golberg, Electron-beam-induced substitutional carbon doping of boron nitride nanosheets, nanoribbons, and nanotubes. ACS Nano **5**, 2916 (2011)
30. V. Meunier, M.B. Nardelli, W. Shelton, C. Roland, J. Bernholc, T. Zacharia, Field emission properties of BN/C and BN@C hybrid nanotubes. MRS Proceedings **739**(H5), 7 (2002)
31. A.N. Enyashin, G. Seifert, A.L. Ivanovskii, Calculation of the electronic and thermal properties of C/BN nanotubular heterostructures. Inorg. Mater. **41**, 595–603 (2005)
32. H. Pan, Y.P. Feng, J. Lin, Boron nitride and carbon double-wall hetero-nanotubes: first-principles calculation of electronic properties. Nanotechnology **19**, 095707 (2008)
33. Z.Y. Zhang, Z. Zhang, W. Guo, Stability and electronic properties of a novel C–BN heteronanotube from first-principles calculations. J. Phys. Chem. C **113**, 13108 (2009)
34. A.N. Enyashin, A.L. Ivanovskii, Mechanical and electronic properties of a C/BN nanocable under tensile deformation. Nanotechnology **16**, 1304 (2005)
35. K.-Y. Xu, E.C. Aifantis, Y.-H. Yan, Vibrations of double-walled carbon nanotubes with different boundary conditions between inner and outer tubes. J. Appl. Mech. **75**(2), 021013 (2008)
36. B. Wu, X.M. Guo, C.Q. Ru, Reduced vibrational frequencies of multiwall carbon nanotubes due to interlayer degrees of freedom. Eur. J. Mech. A/Solids **47**, 206 (2014)
37. S. Arghavan, A.V. Singh, On the vibrations of single-walled carbon nanotubes. J. Sound Vib. **330**, 3102 (2011)
38. L. Boumia, M. Zidour, A. Benzair, A. Tounsi, A Timoshenko beam model for vibration analysis of chiral single-walled carbon nanotubes. Physica E **59**, 186 (2014)
39. R. Ansari, S. Ajori, B. Arash, Vibrations of single- and double-walled carbon nanotubes with layerwise boundary conditions: a molecular dynamics study. Curr. Appl. Phys. **12**, 707 (2012)
40. R. Ansari, S. Ajori, Molecular dynamics study of the torsional vibration characteristics of boron-nitride nanotubes. Phys. Lett. A **378**, 2876 (2014)
41. R. Ansari, R. Gholami, S. Ajori, Torsional vibration analysis of carbon nanotubes based on the strain gradient theory and molecular dynamic simulations. J. Vib. Acoust **135**, 051016 (2013)
42. Y.Y. Zhang, C.M. Wang, V.B.C. Tan, Assessment of Timoshenko beam models for vibrational behavior of single-walled carbon nanotubes using molecular dynamics. Adv. Appl. Math. Mech. **1**, 89 (2009)
43. J. Tersoff, New empirical approach for the structure and energy of covalent systems. Phys. Rev. B **37**, 6991 (1988)
44. D.W. Brenner, Empirical potential for hydrocarbons for use in simulating the chemical vapor deposition of diamond films. Phys. Rev. B **42**, 9458 (1990)
45. K. Albe, W. Muller, K.H. Heinig, Computer simulation and boron nitride. Radiat. Eff. Defects Solids **141**, 85 (1997)
46. K. Albe, W. Muller, Modelling of boron nitride: atomic scale simulations on thin film growth. Comput. Mater. Sci. **10**, 111 (1998)
47. J.E. Lennard-Jones, On the determination of molecular fields. I. From the variation of the viscosity of a gas with temperature. Proc. Royal Soc. A **106**, 441 (1924)
48. A.K. Rappe, C.J. Casewit, K.S. Colwell, W.A. Goddard, W.M. Skiff, UFF, a full periodic table force field for molecular mechanics and molecular dynamics simulations. J. Am. Chem. Soc. **114**, 10024 (1992)
49. M.P. Allen, D.J. Tildesley, *Computer simulation of liquids* (Clarendon, Oxford, 1987)
50. W.G. Hoover, Canonical dynamics: equilibrium phase-space distributions. Phys. Rev. A **31**, 1695 (1985)

51. C.L. Zhang, H.S. Shen, Predicting the elastic properties of double-walled carbon nanotubes by molecular dynamics simulation. J. Phys. D Appl. Phys. **41**, 055404 (2008)
52. P.M. Agrawal, B.S. Sudalayandi, L.M. Raff, R. Komanduri, A comparison of different methods of Young's modulus determination for single-wall carbon nanotubes (SWCNT) using molecular dynamics (MD) simulations. Comput. Mater. Sci. **38**, 271 (2006)
53. S. Timoshenko, *Vibration problems in engineering*, 5th edn. (Wiley, New York, 1990)
54. J.W. Kang, H.J. Hwang, Atomistic study of III-nitride nanotubes. Comput. Mater. Sci. **31**, 237 (2004)
55. M. Griebel, J. Hamaekers, F. Heber, A molecular dynamics study on the impact of defects and functionalization on the Young modulus of boron-nitride nanotubes. Comput. Mater. Sci. **2009**, 45 (1097)
56. L. Jiang, W. Guo, A molecular mechanics study on size-dependent elastic properties of single-walled boron nitride nanotubes. J. Mech. Phys. Solids **59**, 1204 (2011)
57. C. Laurent, E. Flahaut, A. Peigney, The weight and density of carbon nanotubes versus the number of walls and diameter. Carbon **48**, 2994–2996 (2010)